

Supporting Information

A Theoretical Approach to the Study of Thiophene-Based Discotic Systems as Organic Semiconductors

Gregorio García, Mónica Moral, José M. Granadino-Roldán, Andrés Garzón, Amparo

*Navarro, Manuel Fernández-Gómez**

Departamento de Química Física y Analítica. Facultad de Ciencias Experimentales,
Universidad de Jaén. Paraje las Lagunillas, s/n. 23071, Jaén, Spain.

*E-mail: mfg@ujaen.es

Opto-Electronic properties: Optical bandgap. Opto-Electronic properties are related to the optical bandgap, which controls the nature of the electroluminescence signal in light-emitting diodes and the efficiency of light absorption in solar cells.⁷⁴ Experimentally, the optical bandgap is obtained from UV/Vis spectra as the lowest excitation energy from the ground state to the first dipole-allowed excited state. Optical bandgaps (see Table 7S) were estimated only for RO-TriPh by the energy of the HOMO→LUMO transition using TD-DFT. This is to be compared to the lowest, high-oscillator strength transitions involving fully delocalized frontier orbitals as obtained by TD-DFT. Note that the TD-DFT approach only involves properties of the ground state, i.e. the Kohn-Sham orbitals and their corresponding orbital energies obtained in a

ground state calculation. Hence, HOMO → LUMO excitation energies are expressed in terms of ground state properties.⁷⁵ (Note: For references, please see the main body of the article)

Table 5S collects the optical bandgap along with the experimental value reported for the TriPh derivative in (BuO)₆ thin film.²¹ As seen in Table 5S, TD-CAM-B3LYP/6-31G** and TD-B2-PLYP/6-31G** give the smallest deviation respect to the experimental value for RO-TriPh ($\varepsilon_r \sim 2.7\%$), while TD-B3LYP/6-31G** and TD-PW91/6-31G** provide the highest relative errors.

IPs, EAs and Intramolecular Reorganization Energy: Neglecting λ_{outer} , the intramolecular reorganization energy consists of two terms corresponding to the geometry relaxation energies upon going from the neutral-state geometry to the charged-state geometry and *vice versa*:^{1,2}

$$\lambda_i = \lambda_1 + \lambda_2 \quad (1S)$$

λ_1 and λ_2 can be calculated directly from the adiabatic potential energy surface as:

$$\lambda_1 = E^0(G^*) - E^0(G^0) \quad (2S)$$

$$\lambda_2 = E^*(G^0) - E^*(G^*) \quad (3S)$$

where $E^0(G^0)$ and $E^*(G^*)$ are the ground-state energies of the neutral and ionic states, respectively; $E^0(G^*)$ and $E^*(G^0)$ are the energies of the neutral molecule at the optimal ionic geometry and the energy of the ion state at the optimal geometry of the neutral molecule. Once λ_2 is calculated, it is possible to obtain the value of the vertical electron affinity (VEA) and vertical ionization potential (VIP) as:

$$VEA = AEA - \lambda_2^- \quad (4S)$$

$$VIP = AIP + \lambda_2^+ \quad (5S)$$

where AEA and AIP are defined as:⁷²

$$\text{AEA} = E^0(G^0) - E^-(G^-) \quad (6S)$$

$$\text{AIP} = E^+(G^+) - E^0(G^0) \quad (7S)$$

The thermodynamic average of t^2 was obtained through a Boltzmann distribution:

$$\langle t^2 \rangle = \sum_i n_i t_i^2 = \frac{\sum_i t_i^2 \exp(-E_i / kT)}{\sum_i \exp(-E_i / kT)} \quad (8S)$$

n_i is the thermodynamic probability of configuration i at room temperature (300K), with E_i being the relative energy of the rotamer with respect to the global minimum. Eq. (8S) hence allows us to obtain a t value which takes into account all possible hopping pathways between each couple of two stacked discs with different azimuthal angles according to their thermodynamic probability.

Table 1S. HOMO and LUMO levels and HOMO → LUMO excitation energies for RO-TriPh calculated using LR functionals along 6-31G** basis set. Units are in eV.

	CAM-B3LYP	LC-BLYP	LC- ω PBE	Experimental ^a
HOMO	-6.49	-7.41	-7.37	-5.4
LUMO	0.45	1.8	1.62	-1.7
Bandgap (TD)	3.67	4.58	4.44	3.72

^a Taken from reference 21.

Table 2S. Differences between AEA/AIP and LUMO/HOMO energies (eV).

	B3LYP	M06-2X	CAM-B3LYP	PW91	B2-PLYP
AEA + LUMO differences					
RO-TriPh	0.97	-0.63	-0.04	2.01	0.63
RO-BiPhT	1.02	-0.31	0.06	1.63	0.64
RO-TriT	0.96	-0.62	-0.04	1.77	0.55
RO-TetraT	1.33	-0.23	0.23	1.92	0.74
AEA+LUMO differences					
RO-TriPh	-1.00	-0.22	-0.22	-2.17	0.04
RO-BiPhT	-0.63	0.08	0.20	-1.43	0.44
RO-TriT	-1.01	-0.28	-0.23	-1.88	-0.02
RO-TetraT	-0.23	0.53	0.27	-1.05	0.63

Table 3S. HOMO and LUMO energy (eV) levels along with experimental values of RO-TriPh.^a Units are in eV.

Compound	B3LYP		M06-2X		CAM-B3LYP		PW91		B2PLYP		Exp. ^a	
	HOMO	LUMO	HOMO	LUMO	HOMO	LUMO	HOMO	LUMO	HOMO	LUMO	HOMO	LUMO
RO-TriPh	-5.19	-0.47	-6.51	0.13	-6.49	0.45	-4.49	-0.99	-6.05	0.58	-5.4	-1.7
RO-BiPhT	-4.24	-0.59	-5.39	0.03	-5.40	0.33	-3.56	-1.03	-5.02	0.41		
RO-TriT	-4.91	-0.25	-6.21	0.35	-6.24	0.62	-4.17	-0.73	-5.85	0.78		
RO-TetraT	-4.46	-0.21	-5.71	0.50	-5.73	0.68	-3.76	-0.72	-5.40	0.82		

^aTaken from reference 21.

Table 4S. Intramolecular hole (λ_i^+) and electron (λ_i^-) reorganization energies, Ionization Potentials (IP) and Electron Affinities (EA). Units are in eV.

		λ_i^+	AIP	VIP	λ_i^-	AEA	VEA
RO-TriPh	CAM-B3LYP	0.52	6.45	6.83	0.47	-0.67	-0.90
	PW91	0.57	5.88	6.24	0.45	-0.35	-0.80
	B2PLYP	0.58	6.50	6.83	0.38	-1.18	-1.38
RO-BiPhT	CAM-B3LYP	0.60	5.46	5.75	0.96	-0.13	-0.62
	PW91	0.45	5.08	5.31	0.85	0.05	-0.40
	B2PLYP	0.62	5.18	5.49	0.92	-0.39	-0.89
RO-TriT	CAM-B3LYP	0.73	6.19	6.57	1.04	-0.85	-1.36
	PW91	0.66	5.59	5.94	0.85	-0.63	-1.08
	B2PLYP	0.74	5.94	6.32	1.11	-1.15	-1.69
RO-TetraT	CAM-B3LYP	0.33	5.96	6.13	0.93	-0.41	-0.90
	PW91	0.12	5.48	5.54	0.85	0.03	-0.42
	B2PLYP	0.10	5.67	5.73	0.87	-0.33	-0.77

Table 5S. Evolution of the electronic coupling for holes ($|t_{\text{HOMO}}|$) and electrons ($|t_{\text{LUMO}}|$) as a function of the rotational angle (degrees) between neighbouring discs. Electronic couplings are in eV.

	B3LYP			M06-2X			CAM-B3LYP			PW91			B2-PLYP		
	Angle	$ t_{\text{HOMO}} $	$ t_{\text{LUMO}} $												
RO-TriPh	0	0.37	0.38	0.41	0.43	0.41	0.41	0.34	0.34	0.42	0.42	0.44			
	5	0.36	0.36	0.40	0.41	0.40	0.40	0.33	0.32	0.42	0.42	0.42			
	10	0.33	0.32	0.37	0.36	0.37	0.35	0.30	0.28	0.38	0.38	0.37			
	15	0.29	0.25	0.33	0.28	0.32	0.28	0.26	0.22	0.34	0.34	0.29			
	20	0.25	0.15	0.28	0.18	0.28	0.18	0.23	0.14	0.30	0.30	0.18			
	25	0.19	0.09	0.22	0.11	0.22	0.11	0.17	0.08	0.23	0.23	0.11			
	30	0.14	0.03	0.16	0.04	0.16	0.04	0.13	0.03	0.17	0.17	0.04			
	35	0.09	0.01	0.11	0.01	0.11	0.00	0.08	0.01	0.12	0.12	0.01			
	40	0.05	0.03	0.07	0.04	0.07	0.03	0.04	0.03	0.07	0.07	0.04			
	45	0.03	0.04	0.03	0.04	0.04	0.04	0.02	0.03	0.04	0.04	0.04			
	50	0.01	0.03	0.02	0.03	0.01	0.03	0.00	0.02	0.02	0.02	0.03			
	55	0.01	0.03	0.02	0.03	0.01	0.03	0.00	0.02	0.02	0.02	0.03			
	60	0.00	0.00	0.01	0.00	0.01	0.00	0.00	0.00	0.01	0.01	0.00			
	65	0.01	0.03	0.02	0.03	0.01	0.03	0.00	0.02	0.02	0.02	0.03			
	70	0.01	0.03	0.02	0.03	0.01	0.03	0.00	0.02	0.02	0.02	0.03			
	75	0.03	0.04	0.03	0.04	0.04	0.04	0.02	0.03	0.04	0.04	0.04			
	80	0.05	0.03	0.07	0.04	0.04	0.04	0.04	0.03	0.07	0.07	0.04			
	85	0.09	0.01	0.11	0.01	0.04	0.04	0.08	0.01	0.12	0.12	0.01			
	90	0.14	0.03	0.16	0.04	0.07	0.03	0.13	0.03	0.17	0.17	0.04			
RO-BiPhT	0	0.39	0.38	0.43	0.43	0.43	0.42	0.37	0.36	0.45	0.44				
	5	0.38	0.37	0.41	0.41	0.41	0.40	0.35	0.34	0.43	0.42				
	10	0.32	0.31	0.36	0.36	0.36	0.35	0.30	0.29	0.38	0.37				
	15	0.25	0.24	0.27	0.27	0.27	0.26	0.23	0.21	0.28	0.28				
	20	0.15	0.15	0.17	0.17	0.17	0.16	0.14	0.13	0.18	0.18				
	25	0.05	0.06	0.06	0.08	0.06	0.07	0.04	0.05	0.06	0.08				
	30	0.04	0.01	0.04	0.00	0.05	0.00	0.04	0.01	0.04	0.00				
	35	0.13	0.05	0.13	0.05	0.14	0.05	0.12	0.05	0.14	0.05				
	40	0.19	0.06	0.20	0.06	0.20	0.06	0.17	0.06	0.21	0.06				
	45	0.22	0.04	0.24	0.04	0.24	0.04	0.20	0.04	0.25	0.04				
	50	0.23	0.00	0.25	0.01	0.25	0.01	0.21	0.00	0.26	0.01				
	55	0.22	0.05	0.24	0.07	0.24	0.06	0.20	0.04	0.24	0.07				
	60	0.18	0.11	0.20	0.13	0.20	0.12	0.17	0.09	0.21	0.13				
	65	0.14	0.15	0.15	0.17	0.15	0.16	0.12	0.13	0.15	0.16				
	70	0.08	0.16	0.10	0.19	0.10	0.18	0.08	0.15	0.10	0.19				
	75	0.03	0.15	0.04	0.17	0.04	0.17	0.03	0.14	0.05	0.18				
	80	0.01	0.12	0.00	0.13	0.00	0.13	0.01	0.11	0.00	0.14				
	85	0.03	0.06	0.03	0.07	0.03	0.07	0.03	0.06	0.03	0.08				
	90	0.04	0.00	0.04	0.00	0.04	0.00	0.04	0.00	0.04	0.00				
RO-TriT	0	0.41	0.39	0.45	0.49	0.44	0.49	0.39	0.43	0.44	0.45				
	5	0.39	0.35	0.41	0.40	0.40	0.40	0.34	0.32	0.39	0.39				
	10	0.36	0.32	0.37	0.36	0.37	0.38	0.32	0.29	0.36	0.37				
	15	0.32	0.23	0.34	0.30	0.33	0.31	0.28	0.21	0.33	0.30				
	20	0.28	0.15	0.30	0.19	0.30	0.20	0.25	0.12	0.31	0.19				
	25	0.20	0.10	0.21	0.11	0.20	0.11	0.17	0.08	0.20	0.10				
	30	0.12	0.05	0.15	0.06	0.15	0.07	0.10	0.04	0.14	0.07				
	35	0.07	0.02	0.08	0.04	0.09	0.04	0.06	0.00	0.07	0.03				
	40	0.07	0.00	0.06	0.01	0.06	0.01	0.07	0.01	0.08	0.01				
	45	0.08	0.00	0.04	0.01	0.05	0.01	0.07	0.01	0.09	0.01				
	50	0.07	0.00	0.02	0.00	0.02	0.01	0.07	0.01	0.08	0.01				

	55	0.07	0.00	0.01	0.00	0.01	0.00	0.07	0.00	0.08	0.00
	60	0.07	0.00	0.01	0.00	0.01	0.00	0.07	0.00	0.08	0.00
	65	0.07	0.00	0.01	0.00	0.01	0.00	0.07	0.00	0.08	0.00
	70	0.07	0.00	0.02	0.00	0.02	0.01	0.07	0.01	0.08	0.01
	75	0.08	0.00	0.04	0.01	0.05	0.01	0.07	0.01	0.09	0.01
	80	0.07	0.00	0.06	0.01	0.06	0.01	0.07	0.01	0.08	0.01
	85	0.07	0.02	0.08	0.04	0.09	0.04	0.06	0.00	0.07	0.03
	90	0.12	0.05	0.15	0.06	0.15	0.07	0.10	0.04	0.14	0.07
Ro-TetraT	0	0.43	0.39	0.47	0.44	0.48	0.43	0.40	0.36	0.49	0.46
	5	0.43	0.39	0.47	0.44	0.47	0.42	0.39	0.35	0.48	0.45
	10	0.41	0.37	0.45	0.42	0.45	0.41	0.37	0.34	0.46	0.44
	15	0.38	0.35	0.42	0.40	0.42	0.39	0.35	0.32	0.43	0.41
	20	0.34	0.32	0.38	0.37	0.38	0.36	0.31	0.30	0.39	0.38
	25	0.31	0.30	0.33	0.33	0.33	0.32	0.28	0.27	0.34	0.34
	30	0.26	0.26	0.28	0.30	0.28	0.29	0.24	0.23	0.29	0.31
	35	0.20	0.22	0.23	0.26	0.23	0.25	0.19	0.20	0.23	0.27
	40	0.15	0.18	0.17	0.21	0.16	0.21	0.14	0.16	0.17	0.22
	45	0.09	0.14	0.11	0.17	0.10	0.16	0.08	0.12	0.11	0.18
	50	0.04	0.11	0.05	0.13	0.04	0.12	0.03	0.09	0.05	0.14
	55	0.02	0.07	0.01	0.09	0.02	0.09	0.01	0.06	0.01	0.10
	60	0.07	0.04	0.07	0.06	0.07	0.06	0.06	0.03	0.07	0.07
	65	0.11	0.02	0.12	0.04	0.12	0.03	0.10	0.01	0.12	0.04
	70	0.15	0.00	0.16	0.01	0.17	0.01	0.14	0.01	0.17	0.02
	75	0.19	0.01	0.20	0.00	0.21	0.00	0.17	0.02	0.21	0.01
	80	0.21	0.01	0.23	0.00	0.24	0.01	0.20	0.02	0.24	0.00
	85	0.24	0.01	0.26	0.00	0.26	0.00	0.22	0.02	0.26	0.00
	90	0.25	0.00	0.27	0.01	0.28	0.00	0.23	0.01	0.28	0.01

Table 6S. Average values of electronic coupling for holes ($|t_{\text{HOMO}}|$) and electrons ($|t_{\text{LUMO}}|$), calculated mobilities (using $\lambda_{\text{outer}} = 0 \text{ eV}$) for hole and electron hopping motions, relative charge mobilities values for hole and electrons (μ_{rel}^+ and μ_{rel}^-) taking the hole and electron mobilities of RO-TriPh as reference and the ration between hole and electron hopping mobilities ($\mu_{\text{rel}}^+/\mu_{\text{rel}}^-$) calculated at CAM-B3LYP, PW91 and B2-PLYP levels. Charge transfer integrals are in eV, and hopping mobilities are in $\text{cm}^2 \text{ V}^{-1} \text{ s}^{-1}$.

	$ t_{\text{HOMO}} $	$ t_{\text{LUMO}} $	μ^+	μ^-	μ_{rel}^+	μ_{rel}^-
CAM-B3LYP						
RO-TriPh	0.06	0.03	$1.38 \cdot 10^{-2}$	$5.90 \cdot 10^{-3}$	1.00	1.00
RO-BiPhT	0.09	0.07	$1.35 \cdot 10^{-2}$	$1.95 \cdot 10^{-4}$	$9.83 \cdot 10^{-1}$	$3.30 \cdot 10^{-2}$
RO-TriT	0.09	0.04	$3.56 \cdot 10^{-3}$	$2.02 \cdot 10^{-4}$	$2.58 \cdot 10^{-1}$	$3.43 \cdot 10^{-2}$
RO-TetraT	0.13	0.06	$5.83 \cdot 10^{-1}$	$2.38 \cdot 10^{-4}$	42.34	$4.04 \cdot 10^{-2}$
PW91						
RO-TriPh	0.07	0.03	$1.10 \cdot 10^{-2}$	$7.32 \cdot 10^{-3}$	1.00	1.00
RO-BiPhT	0.08	0.06	$5.32 \cdot 10^{-2}$	$4.43 \cdot 10^{-4}$	4.83	$6.06 \cdot 10^{-2}$
RO-TriT	0.08	0.02	$5.84 \cdot 10^{-3}$	$5.06 \cdot 10^{-5}$	$5.31 \cdot 10^{-1}$	$6.91 \cdot 10^{-3}$
RO-TetraT	0.12	0.04	6.37	$2.18 \cdot 10^{-4}$	578.35	$2.98 \cdot 10^{-2}$
B2-PLYP						
RO-TriPh	0.08	0.03	$1.29 \cdot 10^{-2}$	$1.57 \cdot 10^{-2}$	1.00	1.00
RO-BiPhT	0.10	0.07	$1.35 \cdot 10^{-2}$	$2.93 \cdot 10^{-4}$	1.05	$1.86 \cdot 10^{-2}$
RO-TriT	0.10	0.02	$3.96 \cdot 10^{-3}$	$3.52 \cdot 10^{-6}$	$3.06 \cdot 10^{-1}$	$2.24 \cdot 10^{-4}$
RO-TetraT	0.15	0.07	13.24	$5.43 \cdot 10^{-4}$	1023.84	$3.45 \cdot 10^{-2}$

Table 7S. HOMO → LUMO excitation energies (eV) calculated within the isolated molecule approximation along with experimental value for RO-TriPh.

	Bandgap/ eV
TD-B3LYP/6-31G**	3.28
TD-M06-2X/6-31G**	3.49
TD- CAM-B3LYP/6-31G**	3.68
TD-PW91/6-31G**	2.98
TD-B2-PLYP/6-31G**	3.64
Experimental ^a	3.7

^a Taken from reference 21.

Figure 1S. Evolution of relative energy *vs.* rotational angles between discs along stacking axis of a dimer at each essayed level.

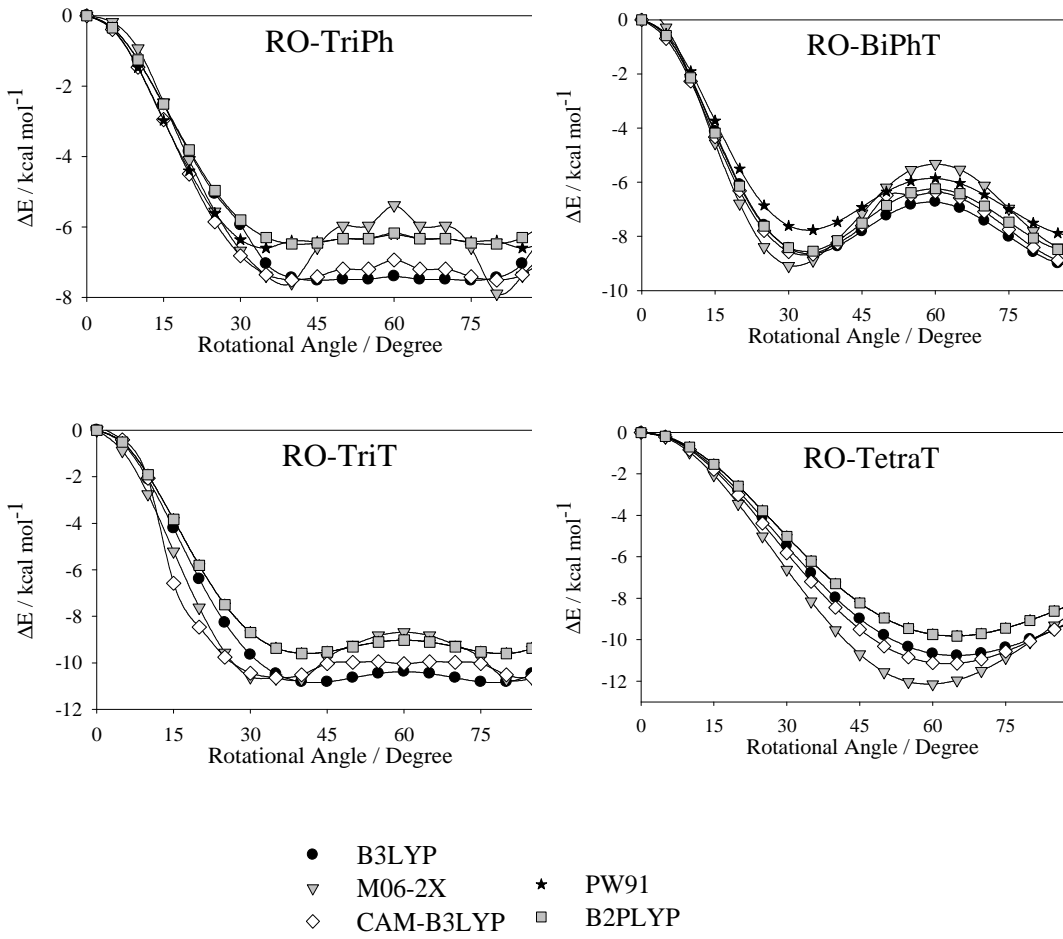


Figure 2S. HOMO and LUMO energy (eV) levels calculated at CAM-B3LYP, PW91 and B2PLYP levels along with experimental values of RO-TriPh (taken from reference 21).

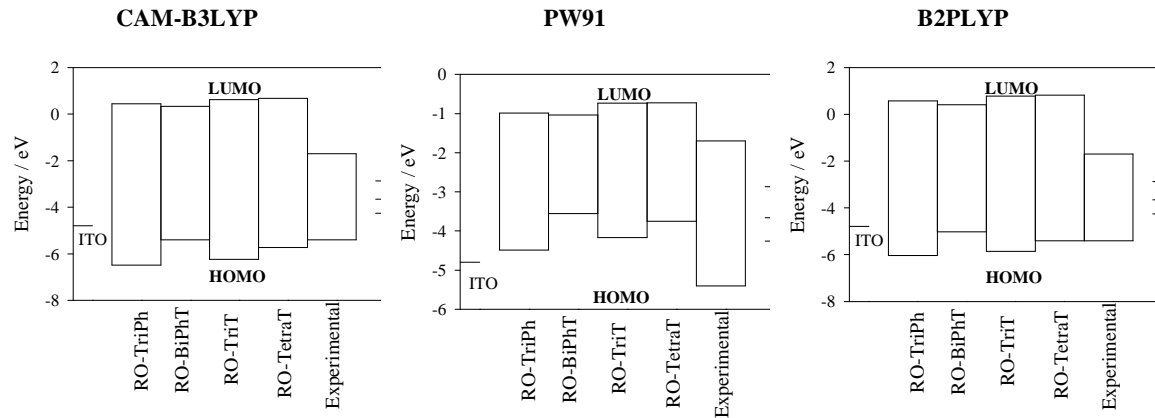


Figure 3S. AIP and AEA levels calculated at CAM-B3LYP, PW91 and B2PLYP levels.

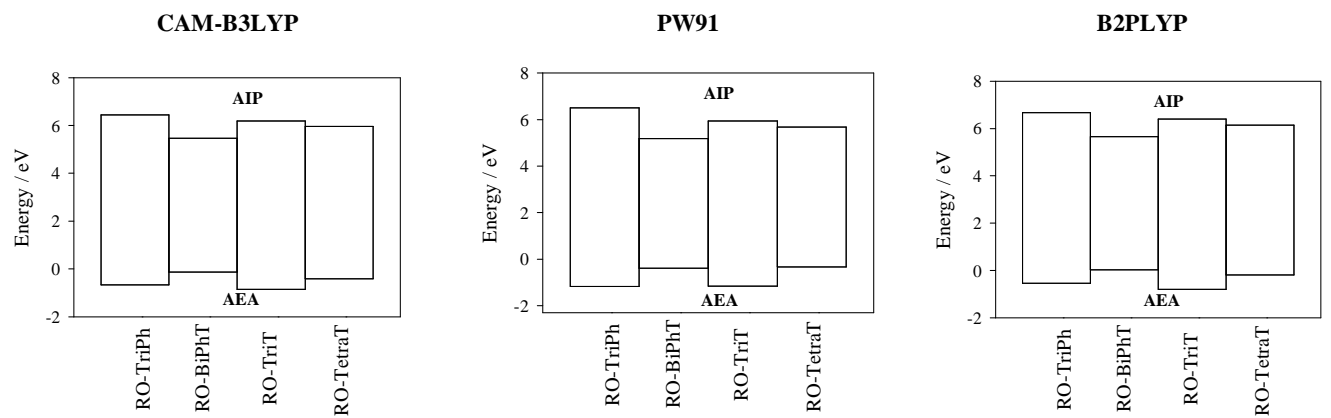


Figure 4S. Evolution of the electronic coupling for holes ($|t_{\text{HOMO}}|$) and electrons ($|t_{\text{LUMO}}|$) as a function of the rotational angle (degrees) between neighbouring discs calculated at M06-2X level. Electronic couplings are in eV.

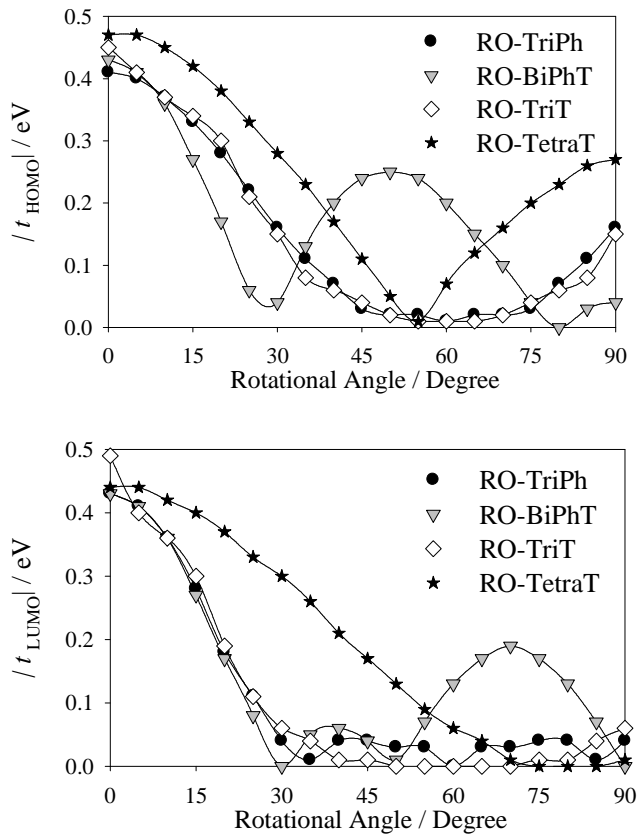


Figure 5S. Evolution of μ^+ with λ_{outer} for RO-TriPh at M06-2X/6-31G** level.

